


Article

Cyclohexene Oxidation with H₂O₂ over Metal-Organic Framework MIL-125(Ti): The Effect of Protons on Reactivity

Nataliya Maksimchuk ^{1,2} , Ji Sun Lee ³, Artem Ayupov ¹, Jong-San Chang ^{3,4} and Oxana Kholdeeva ^{1,2,*}

¹ Borekov Institute of Catalysis, Lavrentieva Ave. 5, Novosibirsk 630090, Russia; nvmax@catalysis.ru (N.M.); artem@catalysis.ru (A.A.)

² Department of Natural Sciences, Novosibirsk State University, Pirogova Str. 2, Novosibirsk 630090, Russia

³ Research group for nanocatalyst, Korea Research Institute of Chemical Technology, Daejeon 34114, Korea; dkagh@kriict.re.kr (J.S.L.); jschang@kriict.re.kr (J.-S.C.)

⁴ Department of Chemistry, Sungkyunkwan University, Suwon 16419, Korea; jschang020@skku.edu

* Correspondence: khold@catalysis.ru; Tel.: +7-383-326-9433

Received: 22 February 2019; Accepted: 22 March 2019; Published: 2 April 2019



Abstract: The catalytic performance of the titanium-based metal–organic framework MIL-125 was evaluated in the selective oxidation of cyclohexene (CyH) with environmentally friendly oxidants, H₂O₂ and ^tBuOOH. The catalytic activity of MIL-125 as well as the oxidant utilization efficiency and selectivity toward epoxide and epoxide-derived products can be greatly improved by acid additives (HClO₄ or CF₃SO₃H). In the presence of 1 molar equivalent (relative to Ti) of a proton source, the total selectivity toward CyH epoxide and *trans*-cyclohexane-1,2-diol reached 75–80% at 38–43% alkene conversion after 45 min of reaction with 1 equivalent of 30% H₂O₂ at 50 °C. With 50% H₂O₂ as the oxidant, the total selectivity toward heterolytic oxidation products increased up to 92% at the same level of alkene conversion. N₂ adsorption, powder X-ray diffraction (PXRD), and infrared (IR) spectroscopy studies before and after the catalytic oxidations confirmed the absence of structural changes in the Metal–organic framework (MOF) structure. MIL-125 was stable toward titanium leaching, behaved as a truly heterogeneous catalyst, and could easily be recovered and reused several times without any loss of the catalytic properties.

Keywords: alkene; epoxidation; heterogeneous catalysis; hydrogen peroxide; metal-organic framework; MIL-125; titanium

1. Introduction

Epoxides are key intermediates used in the manufacture of many valuable bulk and fine chemicals [1–3]. The selective epoxidation of an alkene C=C double bond by stoichiometric amounts of organic peroxy acids or via the chlorohydrin route is widely employed in the industry [1,2]. The development and implementation of greener and more sustainable catalytic epoxidation processes using environmentally benign oxidants is a challenging goal in modern organic syntheses. Hydrogen peroxide is, along with molecular oxygen, the most sought–after oxidant in terms of environmental sustainability because it produces water as its only byproduct [4–6].

It has been widely recognized that titanium-containing molecular sieves are among the best catalysts for selective oxidations with hydroperoxides. Microporous titanium-silicalite TS-1 discovered by the EniChem group has opened a real perspective of H₂O₂ applications in organic synthesis [7–9].

Metal–organic frameworks (MOFs) are currently of great interest due to their potential applications in gas storage and separation, molecular recognition, as well as drug delivery [10–20]. MOFs are also

considered prospective materials for heterogeneous catalysis because of their extremely high surface areas, structural nanoporosity and tunable functionality [21–41]. Another important feature of MOFs is a high content of active metal sites which are uniformly spatially distributed and accessible by reagents, provided the size of the pore entrances allows for the penetration of the reactant molecules [42].

Titanium dioxide, TiO_2 , is considered nowadays one of the most successful photocatalysts due to its high efficiency, chemical stability, abundance, and rather low toxicity. In this context, titanium-based MOFs are viewed as one of the most appealing subclasses of the MOFs family, owing to their promising optoelectronic and photocatalytic properties, including photocatalytic redox reactions, water splitting, and organic pollutant degradation [43–47]. Among the reported Ti-based MOFs, a titanium-oxo-hydroxo-cluster-based MOF MIL-125 is the most studied one since it was the first MOF that revealed photoactivity [48–56]. Moreover, MIL-125 exhibited catalytic activity in the high-pressure cycloaddition of CO_2 to epichlorohydrin and oxidative desulfurization of heterocyclic aromatic sulfur compounds with organic hydroperoxides [57,58]. Recently, some of us demonstrated that MIL-125 reveals a superior selectivity toward *p*-benzoquinones in the oxidation of alkyl-substituted phenols with aqueous H_2O_2 [59,60]. Although the crystal structure of MIL-125 was destroyed under the turnover conditions, the MOF acts as a precursor for the highly active, selective and recyclable catalyst [59,60]. More recently, oxidative desulfurization using H_2O_2 as the oxidant and MIL-125 and MIL-125- NH_2 as catalysts was also reported [61,62], but mesoporous carbons containing TiO_2 nanoparticles obtained by the pyrolysis of MIL-125- NH_2 appeared to be more active than the original MOF [61]. To explore further the potential of MIL-125 for environmentally benign liquid-phase oxidations, we investigated the epoxidation of a representative alkene, cyclohexene, with aqueous hydrogen peroxide and *tert*-butyl hydroperoxide. The aim of this work was not to develop a practical method for the synthesis of epoxides but to clarify factors that govern the catalytic performance of this MOF, comprising well-defined Ti-oxo-hydroxo-clusters. We have found a simple tool that allows alkene epoxidation selectivity to be considerably improved without changes in the MOF crystalline structure.

2. Results and Discussion

2.1. Catalysts Synthesis and Characterization

MIL-125 materials were synthesized by a conventional solvothermal procedure as reported elsewhere [63]. Samples with three different sizes of crystallites (0.5, 1.5, and 5.0 μm) designated as MIL-125-S, MIL-125-M and MIL-125-L, respectively, were prepared using benzoic acid and water as a modulator to alter the particle size [59].

PXRD patterns of the MOF samples given in Figure 1 confirm the quasi-cubic tetragonal structure of MIL-125 built up from cyclic octamers of edge- and corner-sharing $\text{TiO}_5(\text{OH})$ octahedra connected to 12 other cyclic octamers through 1,4-benzenedicarboxylate linkers [48].

Textural parameters of the MIL-125 samples acquired from the N_2 adsorption measurements are presented in Table 1 along with the average particle size estimated by scanning electron microscopy (SEM) (Figure 2). Specific BET surface areas and micropore volumes are close to the characteristic values reported for MIL-125 [48].

Table 1. The physicochemical properties of MIL-125.

Entry	MOF	Particle Size, μm	S_{BET} , m^2/g	V_p , $^a \text{cm}^3/\text{g}$
1	MIL-125-S	0.5	1591	0.59
2	MIL-125-M	1.5	1537	0.58
3			1511	0.57
4	MIL-125-L	5.0	1373 ^b	0.47 ^b

^a Micropore volume calculated by NLDFT; ^b After cyclohexene oxidation with H_2O_2 in the presence of 1 equivalent of HClO_4 (reaction conditions as in Table 2, entry 10).

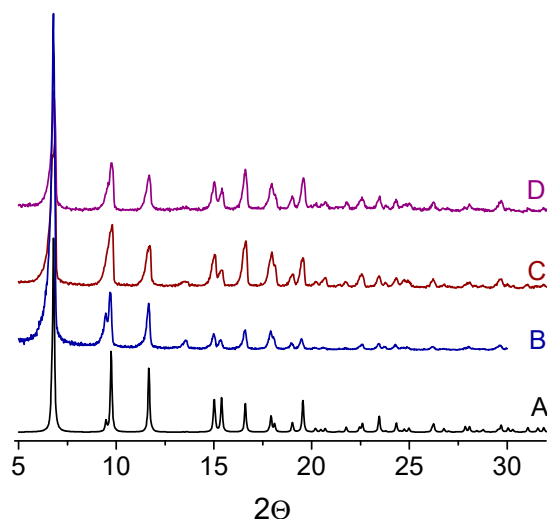


Figure 1. The powder X-ray diffractometry (PXRD) patterns of (A) simulated MIL-125, (B) MIL-125-M, (C) MIL-125-L and (D) MIL-125-L after catalysis (reaction conditions as in Table 2, entry 10).

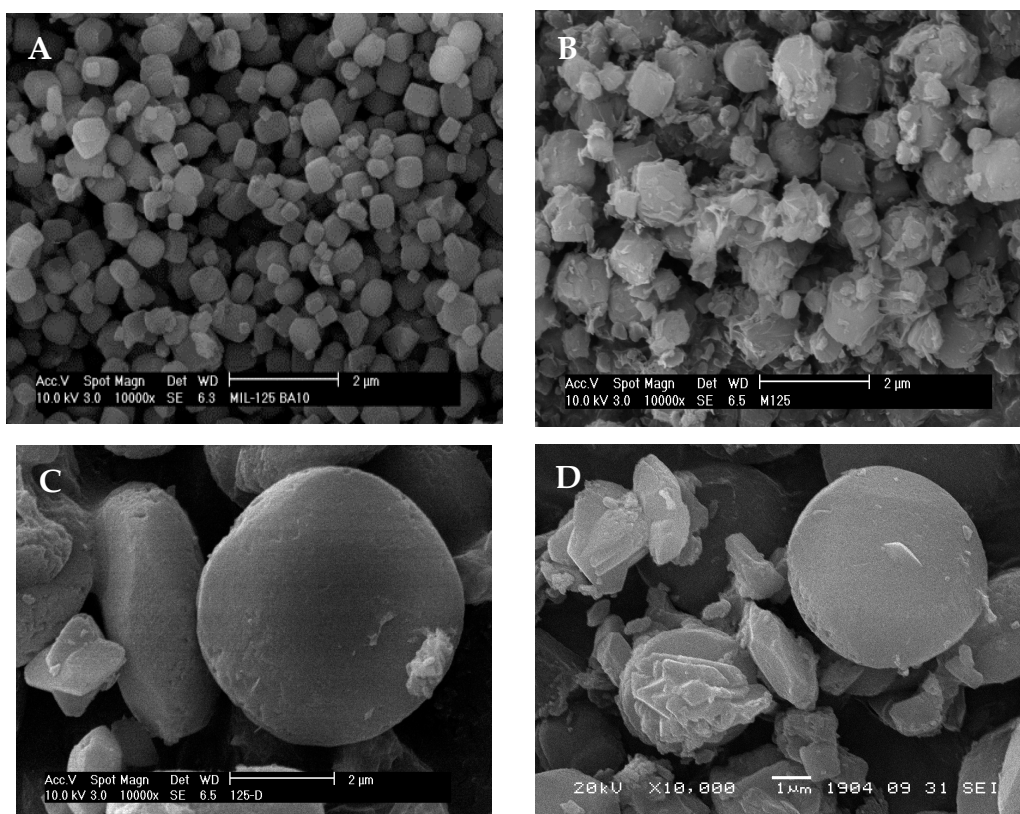


Figure 2. The SEM images of MIL-125 samples: (A) MIL-125-S, (B) MIL-125-M, (C) MIL-125-L, and (D) MIL-125-L after catalysis (reaction conditions as in Table 2, entry 10).

FTIR spectra of MIL-125 (Figure 3, curves A and B) reveal strong characteristic bands of carboxylate groups ($1350\text{--}1700\text{ cm}^{-1}$) and O–Ti–O vibrations ($400\text{--}800\text{ cm}^{-1}$) [48,51,58]. A weak shoulder at the 1710 cm^{-1} characteristic of free terephthalic acid may indicate the presence a minor amount of the free linker within the micropores, while the broad band around 3400 cm^{-1} signifies the presence of intercrystalline water/solvent [48,51,58]. The minor sharp band at 3676 cm^{-1} corresponds to the isolated OH groups of the $\text{TiO}_5(\text{OH})$ clusters.

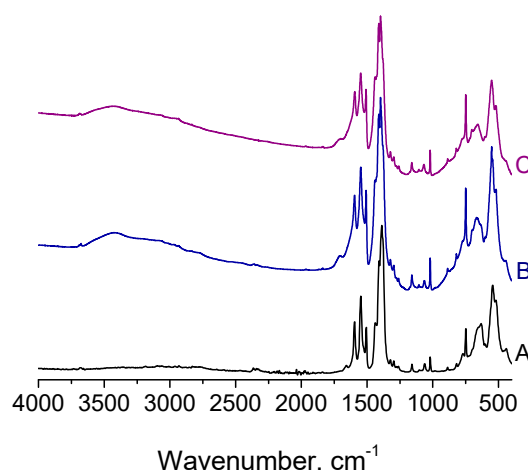


Figure 3. The FTIR spectra of (A) MIL-125-M, (B) MIL-125-L and (C) MIL-125-L after catalysis (reaction conditions as in Table 2, entry 10).

2.2. Catalytic Studies

The catalytic properties of the MIL-125 materials were assessed in cyclohexene (CyH) oxidation with aqueous H_2O_2 in acetonitrile. The main results are collected in Table 2. CyH is one of the most difficult substrates to be epoxidized selectively since it possesses highly reactive H atoms in the allylic position, which can be easily abstracted by radical species to give rise to allylic oxidation products [64].

As compared to the ‘blank’ experiment without any catalyst (Table 2, entry 1), MIL-125 revealed activity in CyH oxidation with 1 equivalent of H_2O_2 (Table 2, entry 3) and produced a set of products that included cyclohexenyl hydroperoxide (HP), 2-cyclohexene-1-ol (enol), 2-cyclohexene-1-one (enone), epoxide, and the epoxide ring opening product *trans*-cyclohexane-1,2-diol (diol). Homolytic (allylic) oxidation products (HP, enol and enone) predominated over heterolytic ones (epoxide and diol), pointing to the homolytic mechanism of H_2O_2 activation.

Table 2. CyH oxidation over MIL-125 ^a.

Entry	Catalyst	T, °C	Time, min	CyH Conv. ^b , %	Product Selectivity ^c , %		
					Epoxide	Diol	Allylic ^d
1	– ^e	50	60	6	16	16	65
2	H^+ ^f	50	60	8	25	26	47
3	MIL-125-M	50	60	26	25	10	60
4	MIL-125-M + 1 eq. H^+	50	45	42	48	27	22
5	MIL-125-M + 1 eq. H^+ ^g	50	45	43	17	63	19
6	MIL-125-M + 1 eq. H^+	30	90	24	63	9	26
7	MIL-125-S + 0.5 eq. H^+ ^h	50	50	30	35	36	28
8	MIL-125-S + 1 eq. H^+	50	45	38	42	34	22
9	MIL-125-S + 1.5 eq. H^+ ⁱ	50	30	41	45	43	9
10	MIL-125-L + 1 eq. H^+	50	45	41	40	38	21

^a Reaction conditions: CyH 0.1 mmol, H_2O_2 0.1 mmol, catalyst 0.01 mmol Ti, $HClO_4$ 0.01 mmol (if any), CH_3CN 1 mL; ^b Maximum achievable conversion. ^c GC yield based on CyH consumed; ^d Total amount of allylic oxidation products (HP + enol + enone) formed; ^e No catalyst was present; ^f Reaction conditions: CyH 0.1 mmol, H_2O_2 0.1 mmol, $HClO_4$ 0.01 mmol, CH_3CN 1 mL; ^g CF_3SO_3H (0.01 mmol) was used as the proton source; ^h $HClO_4$ (0.005 mmol) was added; ⁱ $HClO_4$ (0.015 mmol) was added.

The addition of 1 molar equivalent (relative to Ti atoms in the MOF) of $HClO_4$ increased the reaction rate and attainable CyH conversion (42% conversion in 45 min vs. 26% conversion in 60 min without acid) and significantly changed the product composition, favoring the formation of the heterolytic oxidation products (Table 2, compare entries 3 and 4). CF_3SO_3H produced a similar effect

but also increased the ratio of diol relative to epoxide (Table 2, entry 5). Thus, the total selectivity toward epoxide and diol reached 75–80% in contrast to only 35% without acid additives. It is worthy to note that selectivity to homolytic oxidation products in the ‘blank’ experiment without any catalyst also decreased (from 65 to 47%) upon addition of acid (Table 2, compare entries 1 and 2), but the effect was less pronounced than in the presence of MIL-125 (from 60 to 22%), and the CyH conversion reached only 8% (Table 2, entry 2). Lowering the reaction temperature from 50 to 30 °C reduced the maximum conversion of CyH and changed the ratio between the heterolytic oxidation products, suppressing the diol formation (Table 2, compare entries 4 and 6). With 0.5 equivalent of H⁺, we also observed the rate-accelerating effect and improvement of selectivity, but the levels of conversion and selectivity were lower than with 1 equivalent of acid (Table 2, entries 7 and 8). On the other hand, enlargement of the amount of acid to 1.5 equivalent further increased the reaction rate and practically suppressed the formation of homolytic oxidation products (total selectivity toward epoxide and diol reached 88%; Table 2, entry 9).

Table 3 shows a comparison of the catalytic performance of MIL-125 in the presence of ^tBuOOH, 30% H₂O₂, and 50% H₂O₂. When using ^tBuOOH as an oxidant, the addition of acid also increased the total CyH conversion (46 vs. 25%); however, the amount of homolytic oxidation products did not decrease significantly (45 vs. 54% in the absence of acid) (Table 3, entries 1 and 2). In contrast to the CyH oxidation with H₂O₂, the reaction with ^tBuOOH also produced the product of diol overoxidation, 2-hydroxycyclohexanone. Reducing the amount of water in the reaction system, namely, the use of 50% H₂O₂ instead of 30% H₂O₂, led to a significant growth of the ratio of heterolytic oxidation products (total selectivity 92% vs. 76–78% with 30% H₂O₂) and produced practically no effect on the reaction rate and alkene conversion (Table 3, compare entries 3 and 5 with entries 4 and 6, respectively).

Table 3. The effect of the nature of an oxidant on CyH oxidation over MIL-125 ^a.

Entry	Catalyst	Oxidant	Time, min	CyH Conv. ^b , %	Product Selectivity ^c , %		
					Epoxide	Diol	Allylic ^d
1	MIL-125-M	^t BuOOH	60	25	16	28	54
2	MIL-125-M + 1 eq. H ⁺ ^e	^t BuOOH	45	46	13	17 ^f	45
3	MIL-125-S + 1 eq. H ⁺	30% H ₂ O ₂	45	38	43	33	22
4	MIL-125-S + 1 eq. H ⁺	50% H ₂ O ₂	45	40	57	35	6
5	MIL-125-L + 1 eq. H ⁺	30% H ₂ O ₂	45	41	40	38	21
6	MIL-125-L + 1 eq. H ⁺	50% H ₂ O ₂	45	41	45	47	7

^a Reaction conditions: CyH 0.1 mmol, oxidant 0.1 mmol, catalyst 0.01 mmol Ti, HClO₄ 0.01 mmol (if any), CH₃CN 1 mL; ^b Maximum achievable conversion. ^c GC yield based on CyH consumed; ^d Total amount of allylic oxidation products (HP + enol + enone) formed; ^e CF₃SO₃H (0.01 mmol) was used as proton source; ^f 2-Hydroxycyclohexanone (23% selectivity) was also formed.

In polyoxometallate chemistry, triggering the catalytic activity and/or selectivity by protonation has long been known [65–74]. Thus, Ti(IV)-monosubstituted Keggin phosphotungstate Na_{5-n}H_nPTiW₁₁O₄₀ (n = 2–5) catalyzed H₂O₂-based CyH oxidation to yield diol as the main reaction product, while the Ti-POM with n = 1 produced allylic oxidation products, enol and enone, along with comparable amounts of the corresponding epoxide and diol [67]. Density functional theory (DFT) calculations showed that the formation of epoxide through the Ti–hydroperoxo intermediate is energetically more favorable than through the peroxo intermediate and that the protonation of polyanion is crucial for the activation of the Ti–hydroperoxo species towards heterolytic oxygen-atom transfer because it reduces the corresponding energy barrier [71].

Numerous kinetic and spectroscopic studies implemented on heterogeneous Ti catalysts showed that a hydroperoxo moiety TiOOH and not a peroxo one Ti(η²-O₂) is the species that performs alkene epoxidation with peroxides [8,75–77]. Given that, we may assume that, in the case of MIL-125, the addition of a source of protons also favors the formation of the active TiOOH intermediates responsible for alkene epoxidation.

The structure of MIL-125 has two types of cages, namely, an octahedral one (12.5 Å diameter) and a tetrahedral one (6 Å diameter), accessible through triangular windows of 5–7 Å [48]. In order to elucidate the impact of internal diffusion in the case of MIL-125, samples with different sizes of crystallites (0.5, 1.5, and 5 μm; see Figure 2) have been examined in CyH oxidation with H₂O₂. As one can judge from the kinetic curves shown in Figure 4, the initial rate of CyH oxidation was not affected by the size of the crystallites. Therefore, we may conclude that no diffusion limitation takes place in the course of the catalytic oxidation of CyH over MIL-125. The catalytic properties (CyH conversion and product selectivity) of MIL-125-S and the M and L materials were also close (Table 2, entries 4, 8 and 10).

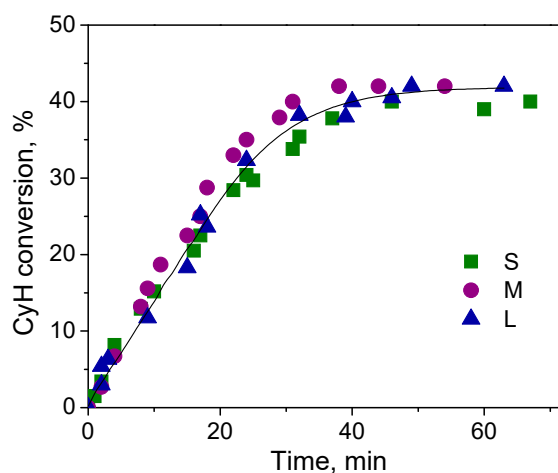


Figure 4. The kinetic curves for CyH oxidation with H₂O₂ over MIL-125 with different particle sizes. Reaction conditions: CyH 0.1 mmol, H₂O₂ 0.1 mmol, catalyst 0.01 mmol Ti, HClO₄ 0.01 mmol, CH₃CN 1 mL, 50 °C.

Incomplete CyH conversions with 1 equivalent of the oxidant may be caused by either blockage of MOF micropores or active sites by the reaction products during the reaction course or unproductive H₂O₂ decomposition competing with the target oxidation reaction. Indeed, the addition of products in the amount close to that found at the end of the reaction (0.015 mmol of epoxide and 0.015 mmol of diol) retarded the oxidation process (Figure 5a), while the addition of water (0.3 mmol)—the product derived from the oxidant—stopped the reaction immediately (Figure 5b), thus indicating that the adsorption of the reaction products could be the reason for catalyst deactivation.

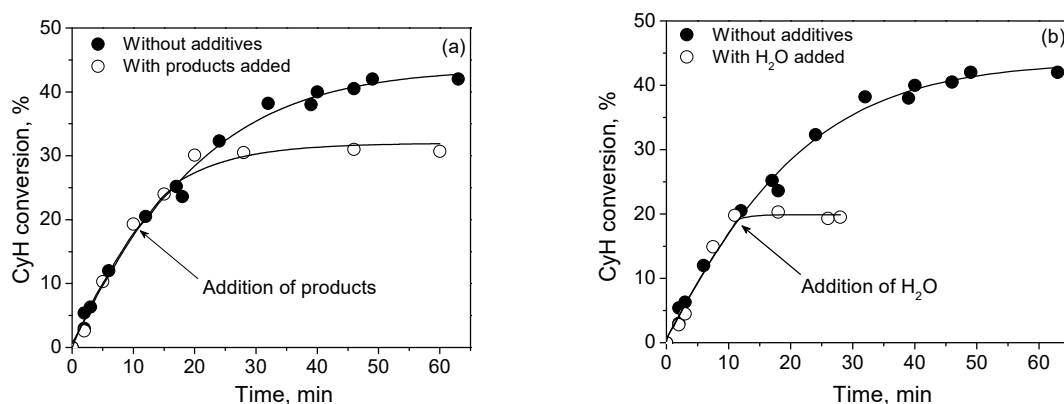


Figure 5. The effect of the addition of reaction products on the course of CyH oxidation with H₂O₂ in the presence of 1 equivalent of HClO₄ over MIL-125-L. Reaction conditions: CyH 0.1 mmol, H₂O₂ 0.1 mmol, catalyst 0.01 mmol Ti, HClO₄ 0.01 mmol, CH₃CN 1 mL, 50 °C, (a) epoxide 0.015 mmol and diol 0.015 mmol or (b) water 0.3 mmol added at ca. 20% CyH conversion.

Another reason for the low CyH conversions could be the high rates of the unproductive decomposition of H_2O_2 relative to the rates of the catalytic oxidation of CyH over MOF, i.e., a rather low efficiency of the oxidant utilization. Indeed, Figure 6 shows that H_2O_2 decomposition over MIL-125 occurs with an appreciable rate. While the target CyH oxidation was strongly accelerated by acid additives, practically no effect was found for H_2O_2 dismutation (Figure 6). The addition of an extra portion of the oxidant (another 0.1 mmol of H_2O_2) after the reaction stopped just slightly increased the CyH conversion (from 41 to 55%). In line with this, iodometric titration confirmed that a significant amount of unreacted H_2O_2 remained at the end of the catalytic reactions both in the presence and in the absence of HClO_4 . With 1 equivalent of H_2O_2 (entry 4, Table 2), conversion of H_2O_2 reached 59% before the reaction stopped, while 61% conversion was attained without acid (entry 3, Table 2). Therefore, H_2O_2 utilization efficiency increased from 45% to 75% due to the addition of protons.

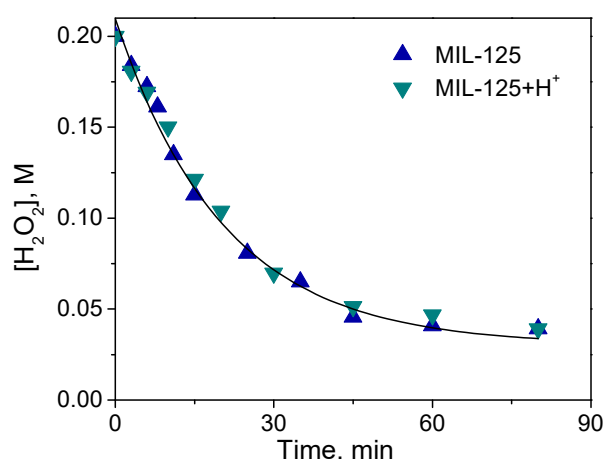


Figure 6. H_2O_2 decomposition in the presence of MIL-125. Reaction conditions: H_2O_2 0.4 mmol, catalyst 0.04 mmol Ti, HClO_4 0.04 mmol (if any), CH_3CN 2 mL, 50 °C.

2.3. Catalyst Recyclability and Stability

The catalyst stability toward leaching of the active species under turnover conditions, as well as the nature of the catalysis, are indispensable properties of solid catalysts, which should be carefully investigated in liquid phase oxidation processes [78]. First of all, we performed a hot filtration test and found a slight increase of CyH conversion after the removal of MIL-125 (Figure 7), which could originate from minor titanium leaching into the solution [78]. However, only a trace amount of titanium (<0.3 ppm) was determined in the filtrate by ICP-AES. This unambiguously proves that the observed catalysis in the presence of MIL-125 is truly heterogeneous, i.e., the reaction occurs on the catalyst surface rather than in the solution as a result of active metal leaching. On the other hand, the slight increase of CyH conversion after the removal of the catalyst might be caused by the accumulation of the radical species in the reaction system due to the thermal decomposition of H_2O_2 [79,80]. Indeed, a similar trend was observed in hot catalyst filtration experiments implemented during the $[\text{Cu}(\text{2-pymo})_2]$ -catalyzed oxidation of tetraline and the MIL-101(Cr)-catalyzed oxidation of propylene glycol, where no active metal species were found in the filtrate [79,80].

MIL-125 could be easily recovered from the reaction mixture by simple filtration, regenerated by washing it with methanol to remove the reaction products adsorbed within the micropores, and reused in, at least, four consecutive runs without the deterioration of its catalytic properties (Table 4). Interestingly, the ratio of heterolytic oxidation products and, in particular, that of epoxide, increased during the recycling, which might be, at least partially, caused by an accumulation of protons in the reaction system during the recycling process.

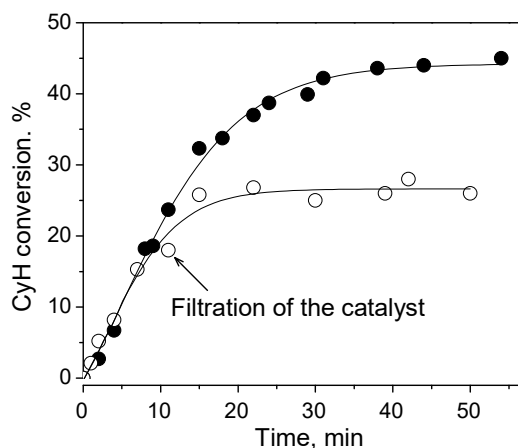


Figure 7. The hot catalyst filtration test for CyH oxidation with H_2O_2 over MIL-125. Reaction conditions as in Table 1, entry 3.

Table 4. The reuse of MIL-125-L in CyH oxidation with H_2O_2 in the presence of 1 equivalent of $HClO_4$ ^a.

Run	CyH Conv., %	Selectivity, %		
		Epoxide	Diol	Allylic ^b
1	41	40	38	21
2	39	42	32	23
3	39	48	28	21
4	40	54	29	14

^a Reaction conditions: CyH 0.1 mmol, H_2O_2 0.1 mmol, catalyst 0.01 mmol Ti, $HClO_4$ 0.01 mmol, CH_3CN 1 mL, 50 °C, 1 h. ^b Sum of allylic oxidation products (HP + enol + enone).

Importantly, there was no decrease in the CyH oxidation rate during the recycling process (Figure 8), which is also consistent with the absence of metal leaching.

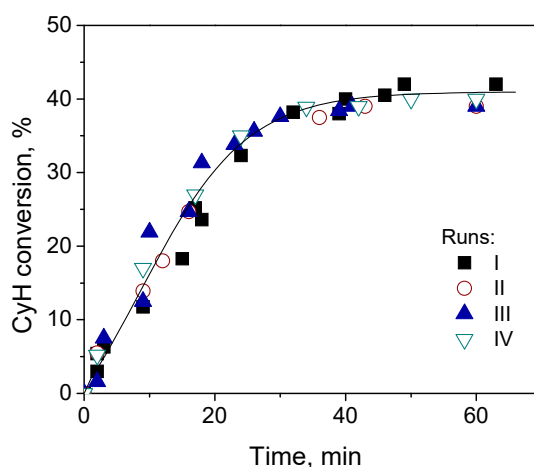


Figure 8. The plots of CyH conversion vs. time in CyH oxidation with H_2O_2 over MIL-125-L in the presence of $HClO_4$. Reaction conditions: CyH 0.1 mmol, H_2O_2 0.1 mmol, catalyst 0.01 mmol Ti, $HClO_4$ 0.01 mmol (added in each run), CH_3CN 1 mL, 50 °C, 1 h.

The stability of the MOF structure under the conditions of CyH oxidation with H_2O_2 was probed by the SEM, N_2 adsorption, PXRD, and FTIR techniques. The shape and size of the MIL-125-L particles remained practically unchanged after catalysis (see Figure 2). In sharp contrast to the previously reported oxidation of alkylphenols with H_2O_2 over MIL-125 (0.4 M H_2O_2 , 80 °C), where the structure

of MIL-125 underwent transformation into an X-ray amorphous mesoporous solid [59], the structure of this MOF retained under the milder conditions used for the CyH oxidation (0.1 M H₂O₂, 50 °C). Indeed, the PXRD pattern of MIL-125-L separated after the catalytic reaction (Figure 1, curve D) completely coincided with that of the initial sample (Figure 1, curve C). The FTIR spectrum of the recovered MOF (Figure 3, curve C) also showed no changes as compared to the spectrum of the fresh sample (Figure 3, curve B). The N₂ adsorption study revealed a minor decrease in the specific surface area and micropore volume of the reused MIL-125-L which might have been caused by adsorption of the reaction products within the pores (Table 1).

3. Materials and Methods

3.1. Materials

Terephthalic acid (98%), titanium isopropoxide (Ti(OiPr)₄, 97%), N,N-dimethylformamide (DMF) and methanol (99.9%) were purchased from Sigma-Aldrich (St. Louis, MO, USA). Acetonitrile (HPLC-grade, Panreac Quimica SLU, Barcelona, Spain) was dried and stored over activated 4 Å molecular sieves. The concentration of H₂O₂ (ca. 30 or 50 wt % in water) and ^tBuOOH (ca. 5.5 M in decane) was determined iodometrically prior to use. Cyclohexene was purchased from Sigma-Aldrich (St. Louis, MO, USA) and purified prior to use by passing it through a column filled with neutral alumina to remove traces of possible oxidation products. All the other compounds were of the best available reagent grade and used without further purification.

3.2. Catalyst Preparation and Characterization

MIL-125 was prepared by a solvothermal method according to the reported protocol [63] using titanium isopropoxide and terephthalic acid in a solvent mixture of DMF and methanol. In a typical synthesis, terephthalic acid (7.6 mmol) and Ti(OiPr)₄ (5.1 mmol) were dissolved in the mixture of DMF (40 mL) and dry methanol (10 mL) and loaded into a three-neck round bottom flask (100 mL), equipped with a reflux condenser at 20 °C. The resulting mixture was crystallized by stirring under reflux conditions at 100 °C for 72 h. After the reaction, the mixtures were allowed to cool down to room temperature, leading to the formation of a white crystalline product in the solution. It was further filtered and then washed with DMF. For further purification, the as-synthesized product was re-dispersed at 60 °C in DMF for 2 h (100 mL of DMF per 1 g of product) and then in methanol for 2 h (100 mL of methanol per 1 g of product). Finally, it was dried overnight at 90 °C under nitrogen. Additionally, MIL-125 samples were dried under vacuum at 130 °C for 6 h prior to use in the catalytic reactions. The particle size of MIL-125 was controlled by the addition of benzoic acid (benzoic acid/Ti(OiPr)₄ molar ratio = 10) as a modulator and the addition of water (H₂O/Ti(OiPr)₄ molar ratio = 1) at the initial mixing of the precursors [59].

3.3. Catalytic Oxidations

Catalytic oxidations were performed under vigorous stirring (600 rpm) in thermostated glass vessels. Typical reaction conditions for CyH oxidation were as follows: CyH 0.1 mmol, H₂O₂ 0.1 mmol, catalyst 2 mg MIL-125 (0.01 mmol Ti), HClO₄ 0.01 mmol (if any), CH₃CN 1 mL, 50 °C. Reactions were started by the addition of H₂O₂. Samples of the reaction mixture were withdrawn periodically during the reaction course by a syringe. The oxidation products were identified by gas chromatography–mass spectrometry (GS–MS). The product yields and substrate conversions were quantified by gas chromatography (GC) using an internal standard, biphenyl. For GC analysis, the method described by Shul'pin was used [81], which involves the treatment of the reaction mixture with PPh₃ in order to reduce the unreacted H₂O₂ and possible organic peroxides formed. Each experiment was reproduced at least 2 times. The concentration of H₂O₂ after the catalytic reaction was determined by iodometric titration. The H₂O₂ utilization efficiency was calculated as the total yield of products based on the oxidant consumed, taking into account the stoichiometric coefficients.

Catalyst reusability was examined in 2–3 time-scaled experiments (the total reaction mixture volume 2–3 mL). After the reactions, the catalyst was filtered off, stirred in 1 mL of methanol for 2 h at 50 °C, filtered off again, dried in air at room temperature and then reused. The nature of catalysis was verified by hot filtration tests.

3.4. Instrumentation

GC analyses were performed using a gas chromatograph Tsvet-500 equipped with a flame ionization detector and a quartz capillary column (30 m × 0.25 mm) filled with DB-5MS (Agilent Technologies, Santa Clara, CA, USA). GC-MS analyses were carried out using an Agilent 7000B system with a triple-quadrupole mass-selective detector Agilent 7000 and a GC Agilent 7890B apparatus (quartz capillary column 30 m × 0.25 mm/HP-5 ms).

Powder X-ray diffraction (PXRD) measurements were performed on a D8 Advance diffractometer (Bruker Corporation, Billerica, MA, USA) equipped with a Vario attachment and Vantec linear PSD, using Cu radiation (40 kV, 40 mA) monochromated by a curved Johansson monochromator (λ Cu $K_{\alpha 1}$ 1.5406 Å).

Infrared spectra were recorded as 0.5–2.0 wt % samples in KBr pellets on a Cary 600 FTIR spectrometer (Agilent Technologies, Santa Clara, CA, USA).

Nitrogen adsorption measurements were carried out at 77 K using an automatic adsorption analyzer Autosorb-6B-Kr instrument (Quantachrome Instruments, Boynton Beach, FL, USA), equipped with 10 Torr absolute pressure transducer, within the partial pressure range 10^{-4} –1.0. The catalysts were degassed at 110 °C for 16 h before the measurements. Surface areas were determined by the BET analysis of low-temperature N₂ adsorption data. Pore size distributions were calculated from the adsorption branches of the nitrogen isotherms by means of the NLDFT method using kernel for nitrogen at 77 K adsorbed on silica with cylindrical pores applied to the adsorption branch of the isotherm. Calculations were made by the ASWin 2.02 software supplied by Quantachrome Instruments (ASWin 2.02, Quantachrome Instruments, Boynton Beach, FL, USA).

Scanning electron microscopy images were acquired by means of a JSM-6460 LV microscope (JEOL Ltd., Tokyo, Japan).

The titanium content in the filtrate, which remained after the separation of the catalysts from the reaction mixture, was determined by ICP-OES using an Optima-430 DV instrument (PerkinElmer Inc., Waltham, MA, USA).

4. Conclusions

The MIL-125 catalyzed the oxidation of cyclohexene using equimolar amounts of H₂O₂ or ^tBuOOH and produced a mixture of products (cyclohexenyl hydroperoxide, 2-cyclohexene-1-ol, 2-cyclohexene-1-one, cyclohexene epoxide and *trans*-cyclohexane-1,2-diol) characteristic of the homolytic mechanism of peroxide activation. The addition of a source of protons (HClO₄ or CF₃SO₃H) in the amount of 1 molar equivalent (relative to Ti) significantly increased the catalytic activity and alkene conversion and changed the product distribution, favoring the formation of heterolytic oxidation products. The effect of protons on the selectivity of epoxidation (the primary reaction en route to diol and ketol) was more significant for H₂O₂ than for ^tBuOOH. With one equivalent of protons, the total selectivity toward epoxide and diol reached 80 and 92% for 30 and 50% H₂O₂, respectively, at 38–43% substrate conversions, while it attained only 52% at a similar conversion when using ^tBuOOH. Moreover, the H₂O₂ utilization efficiency improved from 45 to 75% owing to the addition of protons.

The addition of acid was not critical for the stability of the MOF structure. N₂ adsorption, PXRD, and FTIR studies confirmed the retention of the structural integrity of MIL-125 under the turnover conditions employed for cyclohexene oxidation. MIL-125 did not suffer titanium leaching, behaved as a truly heterogeneous catalyst and could be easily recovered by filtration, regenerated by treatment with methanol and reused at least four times without the loss of catalytic performance.

Author Contributions: N.M. performed catalytic experiments and collected FT-IR spectra. J.S.L. and J.-S.C. provided the catalysts. A.A. performed N₂ adsorption measurements. N.M. and O.K. managed all the experimental work. N.M., O.K. and J.-S.C. managed the writing process.

Funding: This work was supported by Ministry of Science and Higher Education of the Russian Federation (project AAAA-A17-117041710080-4). The research activity was partially supported by the Russian Foundation for Basic Research according to the research project N^o 18-29-04022. J.-S.C. and J.S.L. are grateful to Global Frontier Center for Hybrid Interface Materials (GFHIM) and ISTK for their financial support through the Global Frontier R&D Program and the Institutional Collaboration Research Program (SK-1301).

Acknowledgments: The help of Darya Evtushok in PXRD measurements is greatly appreciated.

Conflicts of Interest: The authors declare no conflict of interest.

References

1. Sheldon, R.A.; van Vliet, M.C.A. Epoxidation. In *Fine Chemicals through Heterogeneous Catalysis*, 1st ed.; Sheldon, R.A., van Bekkum, H., Eds.; Wiley: Weinheim, Germany, 2001; pp. 473–490.
2. Sienel, G.; Rieth, R.; Rowbottom, K.T. Epoxides. In *Ullmann's Encyclopedia of Industrial Chemistry*; Wiley-VCH Verlag GmbH & Co. KGaA: Weinheim, Germany, 2000. [[CrossRef](#)]
3. Dusi, M.; Mallat, T.; Baiker, A. Epoxidation of functionalized olefins over solid catalysts. *Catal. Rev. Sci. Eng.* **2000**, *42*, 213–278. [[CrossRef](#)]
4. *Catalytic Oxidations with Hydrogen Peroxide as Oxidant*; Strukul, G. (Ed.) Kluwer Academic: Dordrecht, The Netherlands, 1992.
5. Jones, C.W. *Application of Hydrogen Peroxide and Derivatives*; Royal Society of Chemistry: Cambridge, UK, 1999.
6. Strukul, G.; Scarso, A. Environmentally benign oxidants. In *Liquid Phase Oxidation via Heterogeneous Catalysis: Organic Synthesis and Industrial Applications*; Clerici, M.G., Kholdeeva, O.A., Eds.; Wiley: Hoboken, NJ, USA, 2013; pp. 1–20.
7. Notari, B. Microporous crystalline titanium silicates. *Adv. Catal.* **1996**, *41*, 253–334.
8. Clerici, M.G.; Domine, M.E. Oxidation reactions catalyzed by transition-metal-substituted zeolites. In *Liquid Phase Oxidation via Heterogeneous Catalysis: Organic Synthesis and Industrial Applications*; Clerici, M.G., Kholdeeva, O.A., Eds.; Wiley: Hoboken, NJ, USA, 2013; pp. 21–93.
9. Buzzoni, R.; Ricci, M.; Rossini, S.; Perego, C. Selective oxidations at Eni. In *Handbook of Advanced Methods and Processes in Oxidation Catalysis*; Duprez, D., Cavani, F., Eds.; Imperial College Press: London, UK, 2014; pp. 353–381.
10. *Functional Metal-Organic Frameworks: Gas Storage, Separation and Catalysis*; Schröder, M. (Ed.) Springer: Heidelberg, Germany, 2010.
11. *Metal-Organic Frameworks: Applications in Separations and Catalysis*; García, H.; Navalón, S. (Eds.) Wiley-VCH Verlag GmbH & Co. KGaA: Weinheim, Germany, 2018.
12. *Elaboration and Applications of Metal-Organic Frameworks, Series on Chemistry, Energy and the Environment*; Ma, S.; Perman, J.A. (Eds.) World Scientific Publishing Co. Pte. Ltd.: Singapore, 2018; Volume 2.
13. Long, J.R.; Yaghi, O.M. The pervasive chemistry of metal-organic frameworks. *Chem. Soc. Rev.* **2009**, *38*, 1201–1508. [[CrossRef](#)]
14. Special Issue on Metal Organic Frameworks. *Micropor. Mesopor. Mater.* **2012**, *157*, 1–146. [[CrossRef](#)]
15. Themed Issue on Metal-Organic Frameworks. *Chem. Soc. Rev.* **2014**, *43*, 5415–6172. [[CrossRef](#)] [[PubMed](#)]
16. Special Issue on Chemistry and Applications of Metal Organic Frameworks. *Coord. Chem Rev.* **2016**, *307*, 105–424.
17. Cluster Issue “Metal-Organic Frameworks Heading towards Application”. *Eur. J. Inorg. Chem.* **2016**, 4265–4529. [[CrossRef](#)]
18. Special Issue on Coordination Polymers/MOFs. *ChemPlusChem* **2016**, *81*, 666–898.
19. Cui, Y.; Li, B.; He, H.; Zhou, W.; Chen, B.; Qian, G. Metal-organic frameworks as platforms for functional materials. *Acc. Chem. Res.* **2016**, *49*, 483–493. [[CrossRef](#)] [[PubMed](#)]
20. Maurin, G.; Serre, C.; Cooper, A.; Férey, G. Metal-Organic Frameworks and Porous Polymers—Current and Future Challenges. special issue on MOFs. *Chem. Soc. Rev.* **2017**, *46*, 3104–3107. [[CrossRef](#)] [[PubMed](#)]

21. Hwang, Y.K.; Férey, G.; Lee, U.-H.; Chang, J.-S. Liquid phase oxidation of organic compounds by metal-organic frameworks. In *Liquid Phase Oxidation via Heterogeneous Catalysis: Organic Synthesis and Industrial Applications*; Clerici, M.G., Kholdeeva, O.A., Eds.; Wiley: Hoboken, NJ, USA, 2013; pp. 371–409.
22. Luz, I.; León, A.; Boronat, M.; Llabres, X.; Corma, A. Selective aerobic oxidation of activated alkanes with MOFs and their use for epoxidation of olefins with oxygen in a tandem reaction. *Catal. Sci. Technol.* **2013**, *3*, 371–379. [[CrossRef](#)]
23. Leus, K.; Liu, Y.-Y.; Van Der Voort, P. Metal-organic frameworks as selective or chiral oxidation catalysts. *Catal. Rev.* **2014**, *56*, 1–56. [[CrossRef](#)]
24. Liu, J.; Chen, L.; Cui, H.; Zhang, J.; Zhang, L.; Su, C.-Y. Applications of metal-organic frameworks in heterogeneous supramolecular catalysis. *Chem. Soc. Rev.* **2014**, *43*, 6011–6061. [[CrossRef](#)] [[PubMed](#)]
25. Gu, Z.-Y.; Park, J.; Raiff, A.; Wei, Z.; Zhou, H.-C. Metal-organic frameworks as biomimetic catalysts. *ChemCatChem* **2014**, *6*, 67–75. [[CrossRef](#)]
26. Kathalikkattil, A.C.; Babu, R.; Tharun, J.; Roshan, R.; Park, D.-W. Advancements in the conversion of carbon dioxide to cyclic carbonates using metal organic frameworks as catalysts. *Catal. Surv. Asia* **2015**, *19*, 223–235. [[CrossRef](#)]
27. Opanasenko, M. Catalytic behavior of metal-organic frameworks and zeolites: Rationalization and comparative analysis. *Catal. Today* **2015**, *243*, 2–9. [[CrossRef](#)]
28. Chughtai, A.H.; Ahmad, N.; Younus, H.A.; Laypkov, A.; Verpoort, F. Metal-organic frameworks: Versatile heterogeneous catalysts for efficient catalytic organic transformations. *Chem. Soc. Rev.* **2015**, *44*, 6804–6849. [[CrossRef](#)]
29. Kholdeeva, O.A. Liquid-phase selective oxidation catalysis with metal-organic frameworks. *Catal. Today* **2016**, *278*, 22–29. [[CrossRef](#)]
30. Panchenko, V.N.; Timofeeva, M.N.; Jhung, S.H. Acid-base properties and catalytic activity of metal-organic frameworks: A view from spectroscopic and semiempirical methods. *Catal. Rev.* **2016**, *58*, 209–307. [[CrossRef](#)]
31. Dhakshinamoorthy, A.; Asiri, A.M.; García, H. Metal-organic frameworks as catalysts for oxidation reactions. *Chem. Eur. J.* **2016**, *22*, 8012–8024. [[CrossRef](#)]
32. He, H.; Perman, J.A.; Zhu, G.; Ma, S. Metal-organic frameworks for CO₂ chemical transformations. *Small* **2016**, *12*, 6309–6324. [[CrossRef](#)] [[PubMed](#)]
33. Rogge, S.M.J.; Bavykina, A.; Hajek, J.; Garcia, H.; Olivos-Suarez, A.I.; Sepurlveda-Escribano, A.; Vimont, A.; Clet, G.; Bazin, P.; Kapteijn, F.; et al. Metal-organic and covalent organic frameworks as single-site catalysts. *Chem. Soc. Rev.* **2017**, *46*, 3134–3184. [[CrossRef](#)]
34. Hu, Z.; Zhao, D. Metal-organic frameworks with Lewis acidity: Synthesis, characterization, and catalytic applications. *CrystEngComm* **2017**, *19*, 4066–4081. [[CrossRef](#)]
35. Liang, J.; Liang, Z.; Zou, R.; Zhao, Y. Heterogeneous catalysis in zeolites, mesoporous silica, and metal-organic frameworks. *Adv. Mater.* **2017**, *29*, 1701139. [[CrossRef](#)] [[PubMed](#)]
36. Dhakshinamoorthy, A.; Asiri, A.M.; Herance, J.R.; García, H. Metal organic frameworks as solid promoters for aerobic autoxidations. *Catal. Today* **2018**, *306*, 2–8. [[CrossRef](#)]
37. Dhakshinamoorthy, A.; Li, Z.; García, H. Catalysis and photocatalysis by metal organic frameworks. *Chem. Soc. Rev.* **2018**, *47*, 8134–8172. [[CrossRef](#)] [[PubMed](#)]
38. Hu, M.-L.; Safarifard, V.; Doustkhah, E.; Rostamnia, S.; Morsali, A.; Nouruzi, N.; Beheshti, S.; Akhbari, K. Taking organic reactions over metal-organic frameworks as heterogeneous catalysis. *Micropor. Mesopor. Mater.* **2018**, *256*, 111–127. [[CrossRef](#)]
39. Qin, J.-S.; Yuan, S.; Lollar, C.; Pang, J.; Alsalme, A.; Zhou, H.-C. Stable metal-organic frameworks as a host platform for catalysis and biomimetics. *Chem. Commun.* **2018**, *54*, 4231–4249. [[CrossRef](#)] [[PubMed](#)]
40. Kramer, S.; Bennedsen, N.R.; Kegnaes, S. Porous organic polymers containing active metal centers as catalysts for synthetic organic chemistry. *ACS Catal.* **2018**, *8*, 6961–6982. [[CrossRef](#)]
41. Dhakshinamoorthy, A.; Asiri, A.M.; Alvaro, M.; García, H. Metal organic frameworks as catalysts in solvent-free or ionic liquid assisted conditions. *Green Chem.* **2018**, *20*, 86–107. [[CrossRef](#)]
42. Maksimchuk, N.V.; Zalomaeva, O.V.; Skobelev, I.Y.; Kovalenko, K.A.; Fedin, V.P.; Kholdeeva, O.A. Metal-organic frameworks of the MIL-101 family as heterogeneous single-site catalysts. *Proc. R. Soc. A* **2012**, *468*, 2017–2034. [[CrossRef](#)]
43. Devic, T.; Serre, C. High valence 3p and transition metal based MOFs. *Chem. Soc. Rev.* **2014**, *43*, 6097–6115. [[CrossRef](#)] [[PubMed](#)]

44. Amador, R.N.; Carboni, M.; Meyer, D. Photosensitive titanium and zirconium metal organic frameworks: Current research and future possibilities. *Mater. Lett.* **2016**, *166*, 327–338. [[CrossRef](#)]
45. Sun, D.; Li, Z. Robust Ti-and Zr-based metal-organic frameworks for photocatalysis. *Chin. J. Chem.* **2017**, *35*, 135–147. [[CrossRef](#)]
46. Assi, H.; Mouchaham, G.; Steunou, N.; Devic, T.; Serre, C. Titanium coordination compounds: From discrete metal complexes to metal–organic frameworks. *Chem. Soc. Rev.* **2017**, *46*, 3431–3452. [[CrossRef](#)]
47. Zhu, J.; Li, P.-Z.; Guo, W.; Zhao, Y.; Zou, R. Titanium-based metal–organic frameworks for photocatalytic applications. *Coord. Chem. Rev.* **2018**, *359*, 80–101.
48. Dan-Hardi, M.; Serre, C.; Frot, T.; Rozes, L.; Maurin, G.; Sanchez, C.; Ferey, G. A new photoactive crystalline highly porous titanium (IV) dicarboxylate. *J. Am. Chem. Soc.* **2009**, *131*, 10857–10859. [[CrossRef](#)] [[PubMed](#)]
49. Zlotea, C.; Phanon, D.; Mazaj, M.; Heurtaux, D.; Guillermin, V.; Serre, C.; Horcajada, P.; Devic, T.; Magnier, E.; Cuevas, F.; et al. Effect of NH₂ and CF₃ functionalization on the hydrogen sorption properties of MOFs. *Dalton Trans.* **2011**, *40*, 4879–4881. [[CrossRef](#)] [[PubMed](#)]
50. Horiuchi, Y.; Toyao, T.; Saito, M.; Mochizuki, K.; Iwata, M.; Higashimura, H.; Anpo, M.; Matsuoka, M. Visible-light-promoted photocatalytic hydrogen production by using an amino-functionalized Ti (IV) metal–organic framework. *J. Phys. Chem. C* **2012**, *116*, 20848–20853. [[CrossRef](#)]
51. Fu, Y.; Sun, D.; Chen, Y.; Huang, R.; Ding, Z.; Fu, X.; Li, Z. An amine-functionalized titanium metal–organic framework photocatalyst with visible-light-induced activity for CO₂ reduction. *Angew. Chem.* **2012**, *124*, 3364–3367. [[CrossRef](#)] [[PubMed](#)]
52. Sun, D.; Ye, L.; Li, Z. Visible-light-assisted aerobic photocatalytic oxidation of amines to imines over NH₂-MIL-125 (Ti). *Appl. Catal. B Environm.* **2015**, *164*, 428–432. [[CrossRef](#)]
53. Santaclara, J.G.; Nasalevich, M.A.; Castellanos, S.; Evers, W.H.; Spoor, F.C.M.; Rock, K.; Siebbeles, L.D.A.; Kapteijn, F.; Grozema, F.; Houtepen, A.; et al. Organic linker defines the excited-state decay of photocatalytic MIL-125 (Ti)-type materials. *ChemSusChem* **2016**, *9*, 388–395. [[CrossRef](#)] [[PubMed](#)]
54. Chambers, M.B.; Wang, X.; Ellezam, L.; Ersen, O.; Fontecave, M.; Sanchez, C.; Rozes, L.; Mellot-Draznieks, C. Maximizing the photocatalytic activity of metal–organic frameworks with aminated-functionalized linkers: Substoichiometric effects in MIL-125-NH₂. *J. Am. Chem. Soc.* **2017**, *139*, 8222–8228. [[CrossRef](#)] [[PubMed](#)]
55. Kampouri, S.; Nguyen, T.N.; Spodaryk, M.; Palgrave, R.G.; Züttel, A.; Smit, B.; Stylianou, K.C. Concurrent photocatalytic hydrogen generation and dye degradation using MIL-125-NH₂ under visible light irradiation. *Adv. Funct. Mater.* **2018**, 1806368. [[CrossRef](#)]
56. Wu, Z.; Huang, X.; Zheng, H.; Wang, P.; Hai, G.; Dong, W.; Wang, G. Aromatic heterocycle-grafted NH₂-MIL-125 (Ti) via conjugated linker with enhanced photocatalytic activity for selective oxidation of alcohols under visible light. *Appl. Catal. B Environm.* **2018**, *224*, 479–487. [[CrossRef](#)]
57. Kim, S.-N.; Kim, J.; Kim, H.-Y.; Cho, H.-Y.; Ahn, W.-S. Adsorption/catalytic properties of MIL-125 and NH₂-MIL-125. *Catal. Today* **2013**, *204*, 85–93. [[CrossRef](#)]
58. McNamara, N.D.; Neumann, G.T.; Masko, E.T.; Urban, J.A.; Hicks, J.C. Catalytic performance and stability of (V) MIL-47 and (Ti) MIL-125 in the oxidative desulfurization of heterocyclic aromatic sulfur compounds. *J. Catal.* **2013**, *305*, 217–226. [[CrossRef](#)]
59. Ivanchikova, I.D.; Lee, J.S.; Maksimchuk, N.V.; Shmakov, A.N.; Chesalov, Y.A.; Ayupov, A.B.; Hwang, Y.K.; Jun, C.-H.; Chang, J.-S.; Kholdeeva, O.A. Highly selective H₂O₂-based oxidation of alkylphenols to *p*-benzoquinones over MIL-125 metal–organic frameworks. *Eur. J. Inorg. Chem.* **2014**, 132–139. [[CrossRef](#)]
60. Kholdeeva, O.A.; Ivanchikova, I.D.; Maksimchuk, N.V.; Mel'gunov, M.S.; Chang, J.-S.; Guidotti, M.; Shutilov, A.A.; Zaikovskii, V.I. Environmentally benign oxidation of alkylphenols to *p*-benzoquinones: A comparative study of various Ti-containing catalysts. *Top. Catal.* **2014**, *57*, 1377–1384. [[CrossRef](#)]
61. Bhadra, B.N.; Song, J.Y.; Khan, N.A.; Jhung, S.H. TiO₂-containing carbon derived from a metal–organic framework composite: A highly active catalyst for oxidative desulfurization. *ACS Appl. Mater. Interfaces* **2017**, *9*, 31192–31202. [[CrossRef](#)] [[PubMed](#)]
62. Zhang, Y.; Lia, G.; Kong, L.; Lu, H. Deep oxidative desulfurization catalyzed by Ti-based metal-organic frameworks. *Fuel* **2018**, *219*, 103–110. [[CrossRef](#)]
63. Vermoortele, F.; Maes, M.; Moghadam, P.Z.; Lennox, M.J.; Ragon, F.; Brouilhou, M.; Biswas, S.; Laurier, K.G.M.; Beurroies, I.; Denoyel, R.; et al. *p*-Xylene-selective metal–organic frameworks: A case of topology-directed selectivity. *J. Am. Chem. Soc.* **2011**, *133*, 18526–18529. [[CrossRef](#)]

64. Sheldon, R.A.; Kochi, J.K. *Metal-Catalyzed Oxidations of Organic Compounds*; Academic Press: New York, NY, USA, 1981.
65. Kholdeeva, O.A.; Maksimov, G.M.; Maksimovskaya, R.I.; Kovaleva, L.A.; Fedotov, M.A. Role of protons in methyl phenyl sulfide oxidation with hydrogen peroxide catalyzed by Ti (IV)-monosubstituted heteropolytungstates. *React. Kinet. Catal. Lett.* **1999**, *66*, 311–317. [[CrossRef](#)]
66. Kamata, K.; Yonehara, K.; Sumida, Y.; Yamaguchi, K.; Hikichi, S.; Mizuno, N. Efficient epoxidation of olefins with $\geq 99\%$ selectivity and use of hydrogen peroxide. *Science* **2003**, *300*, 964–966. [[CrossRef](#)] [[PubMed](#)]
67. Kholdeeva, O.A.; Trubitsina, T.A.; Timofeeva, M.N.; Maksimov, G.M.; Maksimovskaya, R.I.; Rogov, V.A. The role of protons in cyclohexene oxidation with H_2O_2 catalysed by Ti (IV)-monosubstituted Keggin polyoxometalate. *J. Mol. Catal. A Chem.* **2005**, *232*, 173–178. [[CrossRef](#)]
68. Kholdeeva, O.A.; Maksimovskaya, R.I. Titanium- and zirconium-monosubstituted polyoxometalates as molecular models for studying mechanisms of oxidation catalysis. *J. Mol. Catal. A Chem.* **2007**, *262*, 7–24. [[CrossRef](#)]
69. Sartorel, A.; Carraro, M.; Bagno, A.; Scorrano, G.; Bonchio, M. Asymmetric tetraprotonation of $\gamma\text{-}[(SiO_4)W_{10}O_{32}]^{8-}$ triggers a catalytic epoxidation reaction: Perspectives in the assignment of the active catalyst. *Angew. Chem. Int. Ed.* **2007**, *46*, 3255–3258. [[CrossRef](#)]
70. Mizuno, N.; Kamata, K.; Yamaguchi, K. Oxidative functional group transformations with hydrogen peroxide catalyzed by a divanadium-substituted phosphotungstate. *Catal. Today* **2012**, *185*, 157–161. [[CrossRef](#)]
71. Jiménez-Lozano, P.; Ivanchikova, I.D.; Kholdeeva, O.A.; Poblet, J.M.; Carbó, J.J. Alkene oxidation by Ti-containing polyoxometalates. Unambiguous characterization of the role of the protonation state. *Chem. Commun.* **2012**, *48*, 9266–9268. [[CrossRef](#)] [[PubMed](#)]
72. Kholdeeva, O.A. Hydrogen peroxide activation over Ti^{IV} : What have we learned from studies on Ti-containing polyoxometalates? *Eur. J. Inorg. Chem.* **2013**, 1595–1605. [[CrossRef](#)]
73. Satake, N.; Hirano, T.; Kamata, K.; Suzuki, K.; Yamaguchi, K.; Mizuno, N. Synthesis, structural characterization, and oxidation catalysis of a diniobium-substituted silicodecatungstate. *Chem. Lett.* **2015**, *44*, 899–901. [[CrossRef](#)]
74. Maksimchuk, N.V.; Maksimov, G.M.; Evtushok, V.Yu.; Ivanchikova, I.D.; Chesalov, Yu.A.; Maksimovskaya, R.I.; Kholdeeva, O.A.; Solé-Daura, A.; Poblet, J.M.; Carbó, J.J. Relevance of protons in heterolytic activation of H_2O_2 over Nb(V): Insights from model studies on nb-substituted polyoxometalates. *ACS Catal.* **2018**, *8*, 9722–9737. [[CrossRef](#)]
75. Yoon, C.W.; Hirsekorn, K.F.; Neidig, M.L.; Yang, X.; Tilley, T.D. Mechanism of the decomposition of aqueous hydrogen peroxide over heterogeneous TiSBA15 and TS-1 selective oxidation catalysts: Insights from spectroscopic and density functional theory studies. *ACS Catal.* **2011**, *1*, 1665–1678. [[CrossRef](#)]
76. Bordiga, S.; Groppo, E.; Agostini, G.; van Bokhoven, J.A.; Lamberti, C. Reactivity of surface species in heterogeneous catalysts probed by in situ X-ray absorption techniques. *Chem. Rev.* **2013**, *113*, 1736–1850. [[CrossRef](#)] [[PubMed](#)]
77. Kholdeeva, O.A.; Ivanchikova, I.D.; Maksimchuk, N.V.; Skobelev, I.Y. H_2O_2 -based selective epoxidations: Nb-silicates versus Ti-silicates. *Catal. Today* **2018**. [[CrossRef](#)]
78. Sheldon, R.A.; Wallau, M.; Arends, I.W.C.E.; Schuchardt, U. Heterogeneous catalysts for liquid-phase oxidations: Philosophers' stones or Trojan horses? *Acc. Chem. Res.* **1998**, *31*, 485–493. [[CrossRef](#)]
79. Llabres, X.; Casanova, O.; Galiasso Tailleur, R.; Garcia, H.; Corma, A. Metal organic frameworks (MOFs) as catalysts: A combination of Cu^{2+} and Co^{2+} MOFs as an efficient catalyst for tetralin oxidation. *J. Catal.* **2008**, *255*, 220–227. [[CrossRef](#)]
80. Torbina, V.V.; Ivanchikova, I.D.; Kholdeeva, O.A.; Skobelev, I.Y.; Vodyankina, O.V. Propylene glycol oxidation with *tert*-butyl hydroperoxide over Cr-containing metal-organic frameworks MIL-101 and MIL-100. *Catal. Today* **2016**, *278*, 97–103. [[CrossRef](#)]
81. Shul'pin, G.B. Metal-catalyzed hydrocarbon oxygenations in solutions: The dramatic role of additives: A review. *J. Mol. Catal. A* **2002**, *189*, 39–66. [[CrossRef](#)]

